



ISPRAS OPEN Moscow 2019

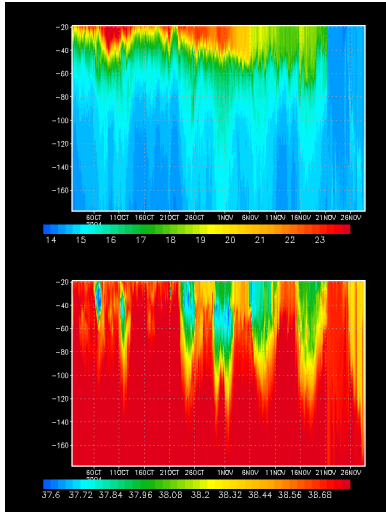
Identification of turbulent model parameters in ocean surface models

Turboradar / Turbident / Urbarisq

C. Aldebert, M. Baklouti, D. Bourras, H. Branger, T. Caby, J.L. Devenon, D. Faranda, P. Fraunié, R. Fuchs, P. Garreau, G. Koenig, I. Pairaud, V. Rey, A. Sentchev, V. Shrira, S. Vaienti



Surface layer problem



284

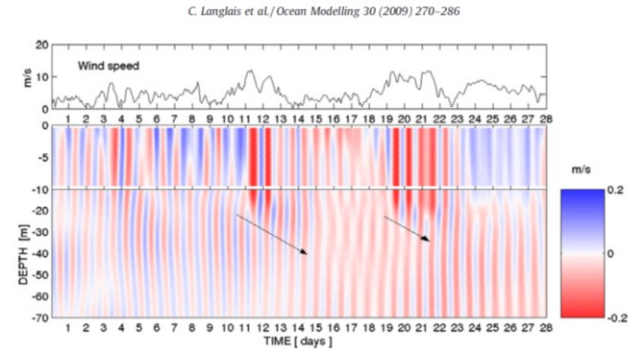


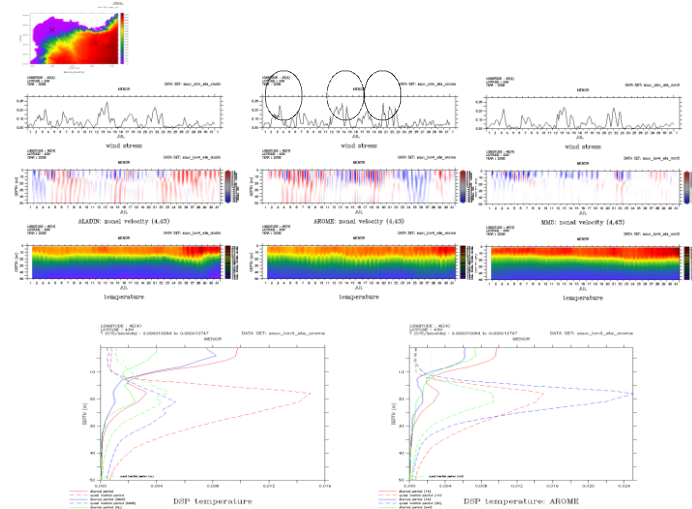
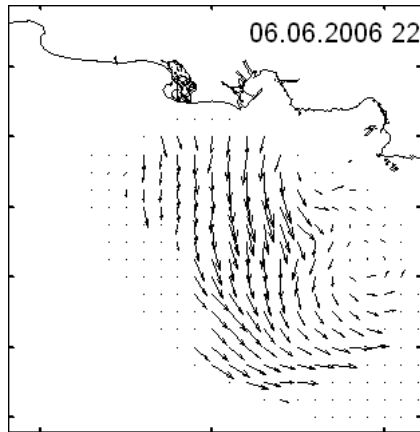
Fig. 19. Time evolution of the wind speed and of the vertical profile of the zonal current at 3.1°E/42.6°N during a 28 day period in summer, in a simulation with the GoL64 ocean circulation model driven with REMO forcing

Internal waves permitting models: summer 2008

Langlais et al, 2009, Schaeffer et al 2010

Gliders observations

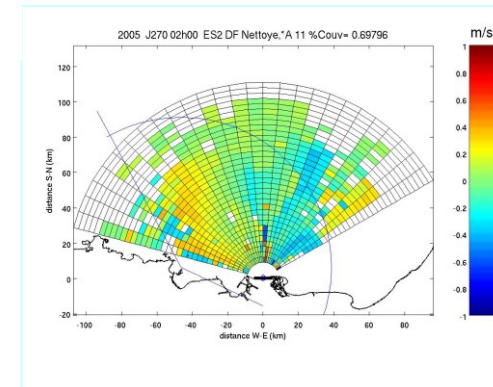
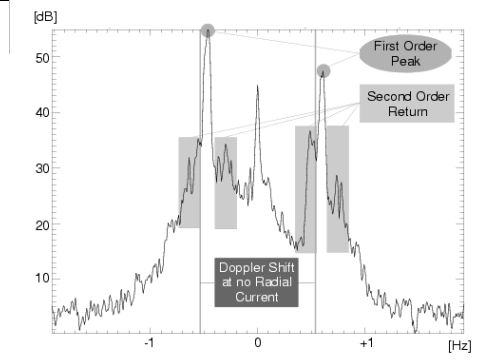
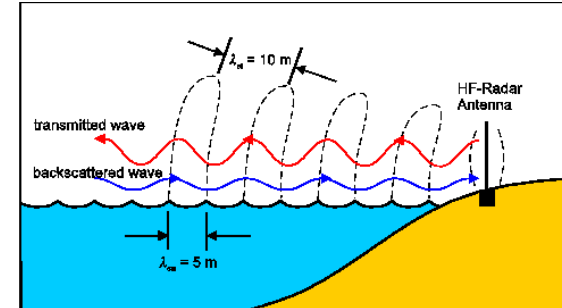
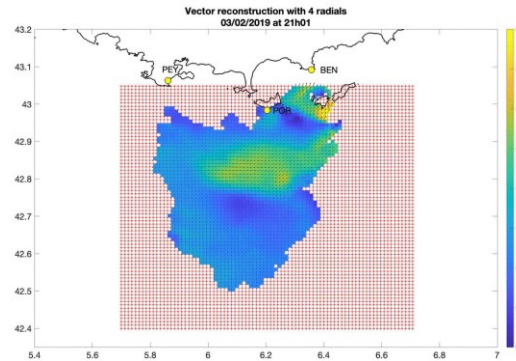
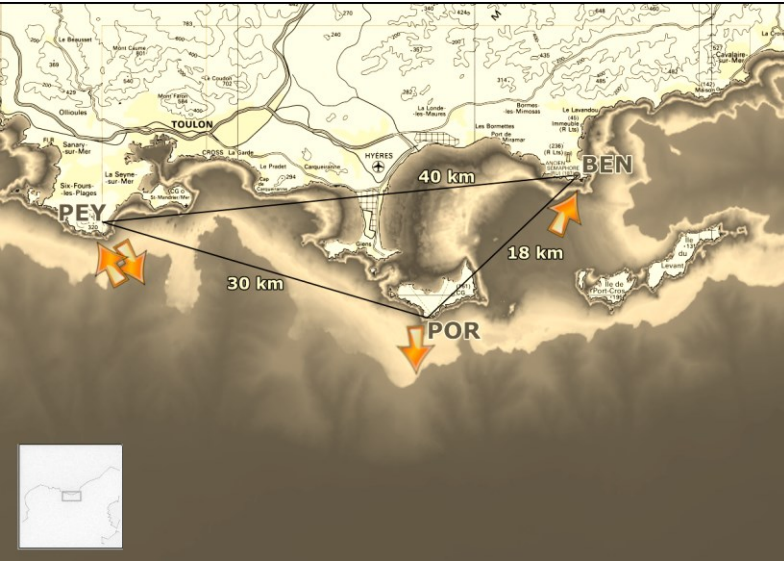
(Testor et al, 2008)



HF radars observations

(Forget & Shrira, 2015)

HF radars H current mapping

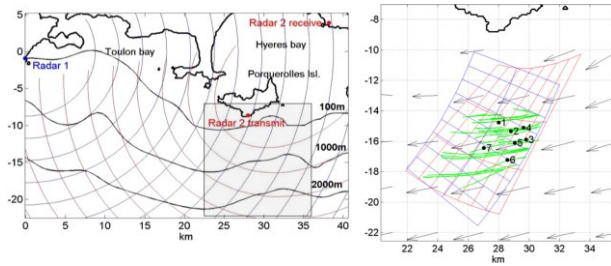
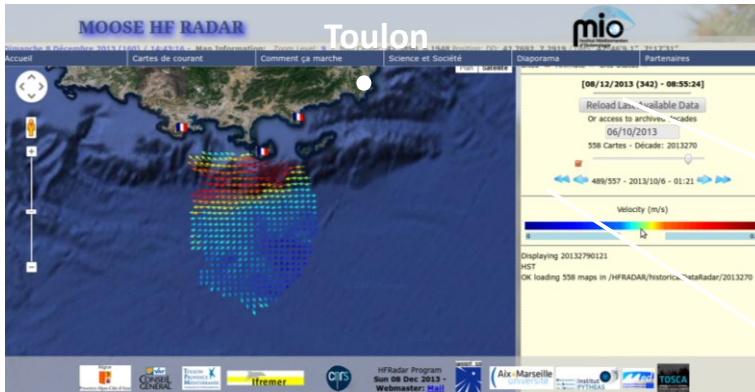


**M.I.O. HF Radar team : C. A. Guérin (PR), C. Quentin(IR),
A. Gramoullé (IE), D. Dumas(IE), B. Zakardjian(PR), A. Molcard (PR),
M. Saillard (PR)**

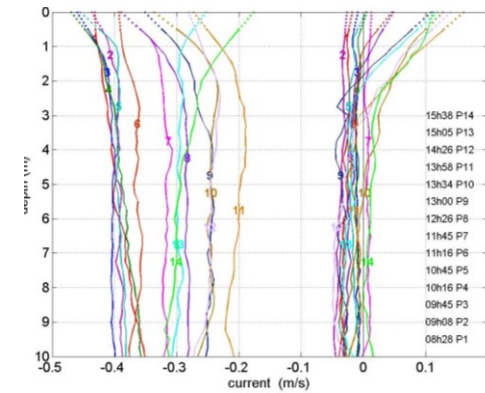
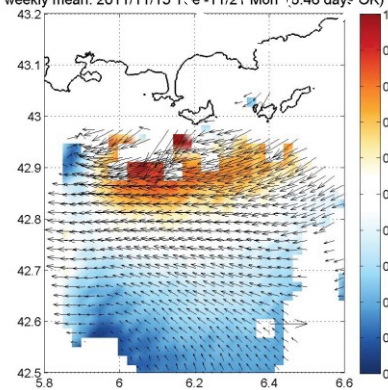
MOOSE / EU MARITTIMO SICOMAR PLUS / ANR TURBIDENT

SUBCORAD campaign 2013

Sentchev, Forget, Fraunié, 2015



weekly mean: 2011/11/15 1.0e -11/21 Mon (3.46 days OK)



The Ekman (1905) solution

$$\frac{\partial u}{\partial t} - fv = \nu_t \frac{\partial^2 u}{\partial z^2}$$

$$\frac{\partial v}{\partial t} + fu = \nu_t \frac{\partial^2 v}{\partial z^2}$$

Steady solution

$$\begin{cases} U(z) = \text{sign}(f) U_c \sqrt{2} \exp\left(-\frac{z}{d_B}\right) \cos\left(\frac{\pi}{4} - \frac{z}{d_B}\right) \\ V(z) = U_c \sqrt{2} \exp\left(-\frac{z}{d_B}\right) \sin\left(\frac{\pi}{4} - \frac{z}{d_B}\right) \end{cases}$$

de solution de la spirale

d'Ekman est:

$$\begin{cases} u = u_g (1 - e^{-\gamma z}) \cos(\gamma z) \\ v = u_g e^{-\gamma z} \sin(\gamma z) \end{cases}$$

$$\text{où } \gamma = \left(\frac{f}{2K}\right)^{1/2}$$

$$\text{où } K = \nu$$

11-4 EKMAN'S Planetary Boundary Layer Solution 429

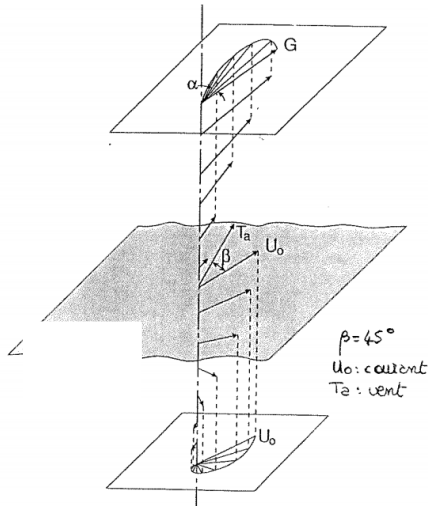


Figure 11-6 Sketch of velocity vectors in the adjacent atmospheric and oceanic PBLs. Note the change in scales.

unsteady solution

$$\begin{cases} U(z,t) = \frac{2 \tau_{sy}}{\rho_r d_B f} \int_0^{\bar{t}} \frac{\sin(2 \pi \zeta)}{\sqrt{\zeta}} \exp\left(-\frac{z^2}{4 \pi d_B^2 \zeta}\right) d\zeta \\ V(z,t) = \frac{2 \tau_{sy}}{\rho_r d_B |f|} \int_0^{\bar{t}} \frac{\cos(2 \pi \zeta)}{\sqrt{\zeta}} \exp\left(-\frac{z^2}{4 \pi d_B^2 \zeta}\right) d\zeta \end{cases}$$

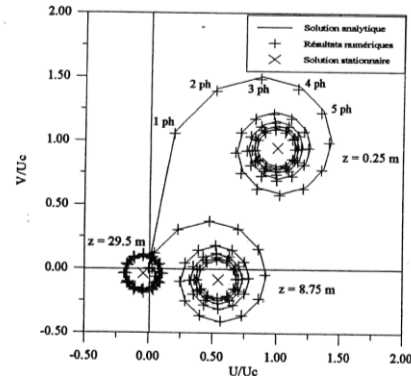
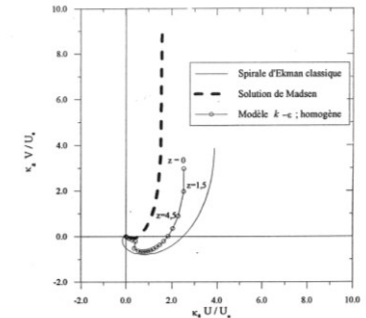


Fig. 21- A l'état stationnaire, évolution en fonction de la profondeur du vecteur vitesse obtenu avec le modèle k-ε, chaque point représente le vecteur vitesse à une profondeur z (m) indiquée sur les premiers points.



K-ε model (C. Verdier-Bonnet 1996, 1999)

Ekman layer inflectional Instability

- Ekman Spiral (Ekman 1905, Gonella 1971, Madsen 1977, Lewis&Belcher 2004, Elipot&Gille 2009, Almela&Shrira sub)
- Stability analysis (Faller 1965, Brown 1974, Leibovich & Lele, 1985)
- LES (Deardorff 1970, 1972, Mason & Thomson 1987, Moeng&Sullivan 1994, Zikanov et al, 2003, Sullivan&McWilliams 2010)
- DNS (Coleman, Ferziger, Spalart, 1990)
- Observations PBL (Le Mone 1973)
- Observations Ocean (Price et al 1987, 1999, Csanady 2001)

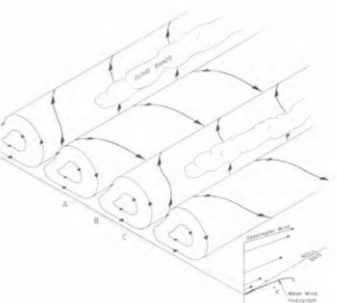


Figure 11.18 Sketch of the PBL containing large eddies. Typical secondary flow (modified Ekman layer).

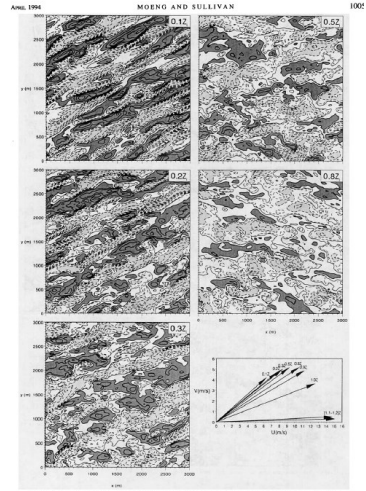


FIG. 3. Contours of α in the $x-y$ plane at five height levels for simulation 3 and its visual analog (contours (-3, -2.5, -2, -1.5, -1, -0.5), (0), (0.5, 1, 1.5, 2, 2.5), dark (light) shading refers to α (contour) from 0.5 (-0.5).

Moeng&Sullivan 1994

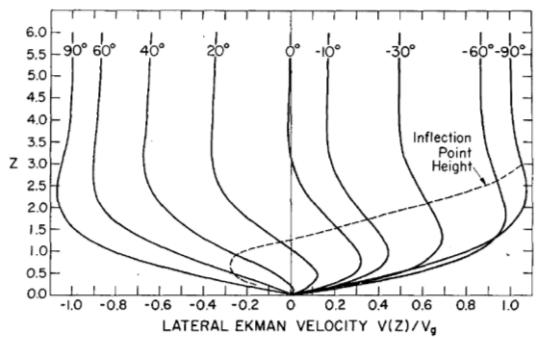


FIG. 1. Two-dimensional velocity profiles taken in vertical planes normal to the roll direction. The angle ϵ denotes the roll angle to the left of the geostrophic velocity. The height and velocity are given in increments of δ and V_g , respectively.

Brown 1972

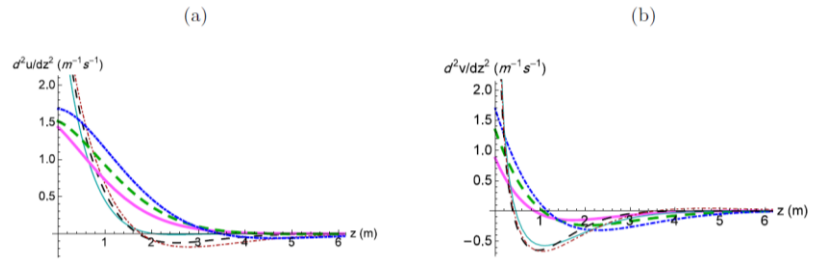
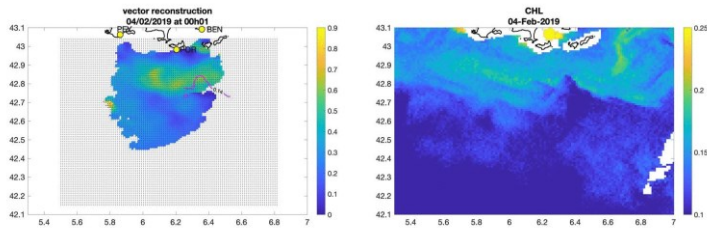


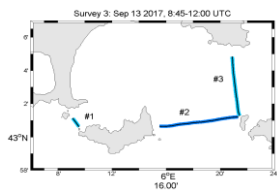
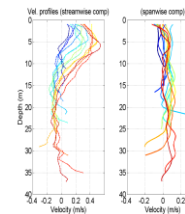
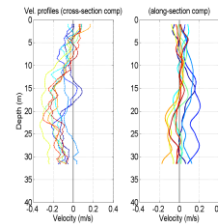
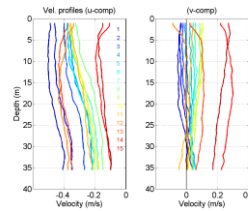
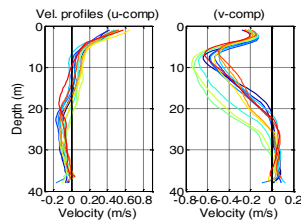
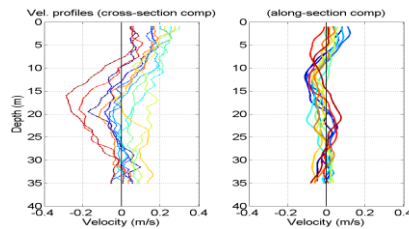
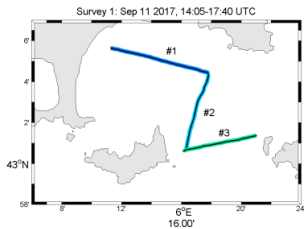
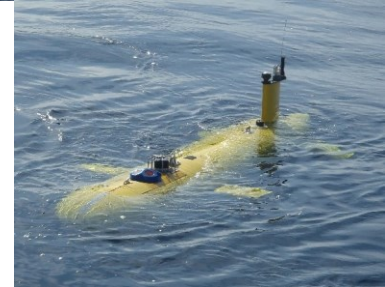
FIGURE 6. Second derivatives of the velocity profiles in two models of viscosity (the classical Ekman model (thick lines) and time-dependent viscosity model (thin lines)) at different times: $\tilde{t} = 2$ (solid lines), $\tilde{t} = 3$ (dashed lines) and $\tilde{t} = 5$ (dotted lines). (a) The second derivative of x -component. (b) The second derivative of y -component. The parameters: $\delta = 3$ hrs, $f = 10^{-4} s^{-1}$, $\nu_0 = 10^{-4} m^2 s^{-1}$.

Almela & Shrira sub

TURBIDENT campaign 2018



Dumas, Granoullé & Guérin



D. Bourras, H. Branger, A. Sentchev

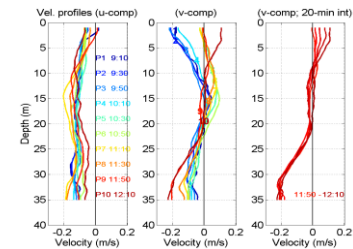
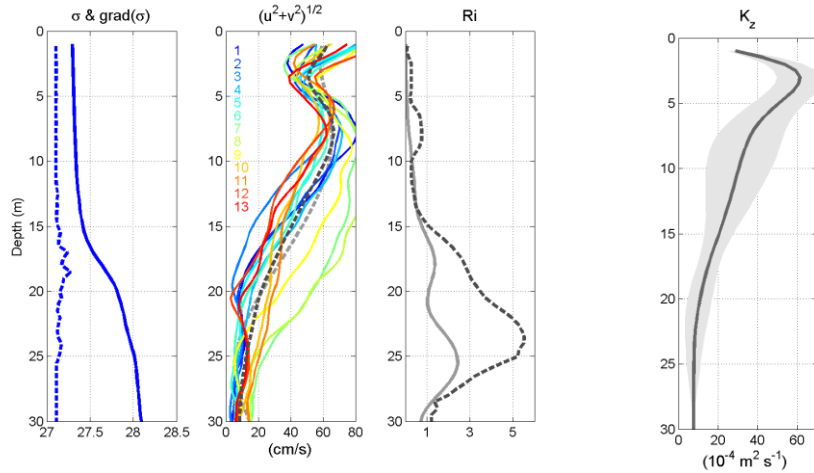
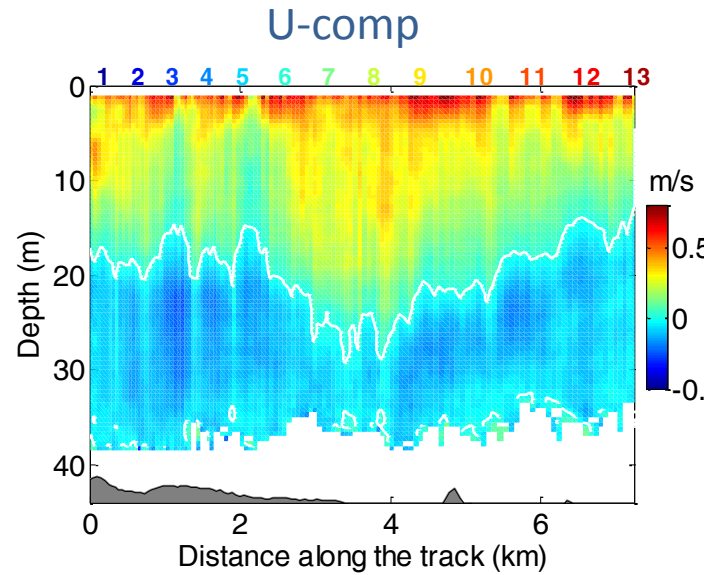
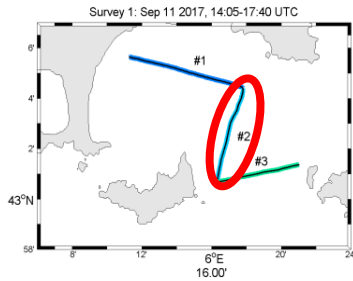


Table 1. Overview of optimization methods, and their pros and cons when applied to complex geophysical models that are costly to program and run. We do not mention Kalman methods, which cannot be used for parameter identification in their current form (Sun et al., 2016).

Type	Method	Pros	Cons
By-hand		Easy, only model runs.	Need many runs, unlikely to succeed without a method.
Stochastic, global	Simulated-Annealing	Generic, easy to implement, noisy data.	Need many runs, even for a few parameters.
	Genetic algorithms	Generic, many parameters, noisy data.	Need many runs, hard to tune.
	Hamiltonian Monte-Carlo	Generic, Bayesian framework.	Need many runs
Local gradient descent	Adjoint	Cheap to run, explicit gradient, many parameters.	Costly to build, problem-specific, noise-sensitive.
	Finite-Difference	Generic, easy to implement, almost exact gradient.	Number of runs proportional to the number of parameters, noise-sensitive.
	Simultaneous Perturbation Stochastic Approximation	Generic, easy to implement, cheap to run, many parameters, less noise-sensitive.	Approximative gradient.

Eddy viscosity estimate



From 1 D Ekman model (A Sentchev)

Classical standard values of TKE turbulent closure model parameters

Table 2. Model parameters. Gaspar et al. (1990)

Parameter	Value	Unit	Meaning
c_k	0.1	-	TKE constant (eddies diffusivity)
c_ϵ	0.7	-	TKE constant (turbulent dissipation)
$K_{m_{\min}}$	$3 \cdot 10^{-5}$	$\text{m}^2 \cdot \text{s}^{-1}$	minimal value for moment diffusivity
\bar{e}_{\min}	$2 \cdot 10^{-6}$	$\text{m}^2 \cdot \text{s}^{-2}$	minimal value for TKE
$\bar{e}_{\min 0}$	10^{-4}	$\text{m}^2 \cdot \text{s}^{-2}$	minimal value for TKE at surface
Pr_t	1	-	Prandtl number
K_{ratio}	1	-	ratio between TKE and momentum diffusivities
bb	3.75	-	constant to compute surface TKE from wind stress

Simple hydrodynamic model 1DV

- T temperature ; S salinity ; $\mathbf{U}=(u,v)$ and w horizontal and vertical velocity , I solar irradiance, F_{sol} solar constant, c_p specific heat.

$$\frac{\partial \bar{T}}{\partial t} = \frac{F_{\text{sol}}}{\rho_0 c_p} \frac{\partial I}{\partial z} - \frac{\partial \overline{T'w'}}{\partial z},$$

$$\frac{\partial \bar{S}}{\partial t} = - \frac{\partial \overline{S'w'}}{\partial z},$$

$$\frac{\partial \mathbf{U}}{\partial t} = -f\mathbf{k} \times \mathbf{U} - \frac{\partial \overline{\mathbf{U}'w'}}{\partial z},$$

Turbulent closure scheme

Eddy diffusivities: K_h , K_s , K_m

$$\overline{T'w'} = -K_h \frac{\partial \bar{T}}{\partial z}, \quad \overline{S'w'} = -K_s \frac{\partial \bar{S}}{\partial z}, \quad \overline{U'w'} = -K_m \frac{\partial \bar{U}}{\partial z},$$

$$K_m = \max \left(K_{m_{\min}}, c_k l_k \sqrt{\bar{e}} \right),$$

$$K_s = K_h = \frac{K_m}{Pr_t},$$

Turbulent closure scheme

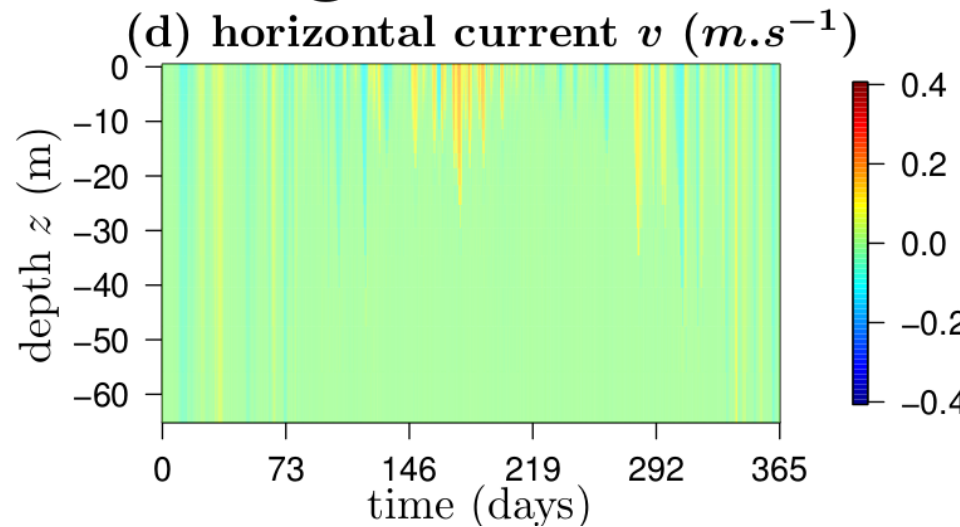
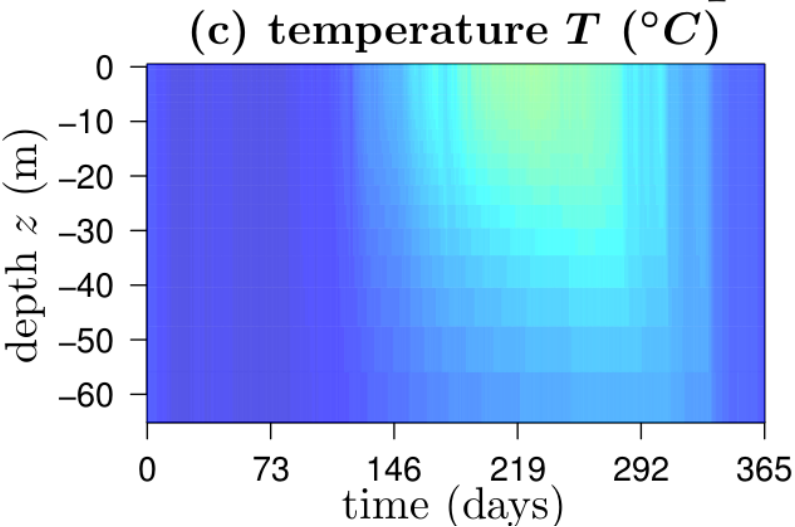
$$\bar{e} = 0.5(\overline{u'^2} + \overline{v'^2} + \overline{w'^2}) \quad \varepsilon = c_\varepsilon \frac{\bar{e}^{3/2}}{l_\varepsilon},$$

$$\frac{\partial \bar{e}}{\partial t} = \frac{\partial}{\partial z} \left(K_e \frac{\partial \bar{e}}{\partial z} \right) - \overline{\mathbf{U}'w'} \cdot \frac{\partial \mathbf{U}}{\partial z} + \overline{b'w'} - \varepsilon$$

$$\bar{e}_{(z=0)} = \max \left(\bar{e}_{\min 0}, bb \frac{\sqrt{\tau_x^2 + \tau_y^2}}{\rho} \right)$$

Optimization : arbitrary starting state

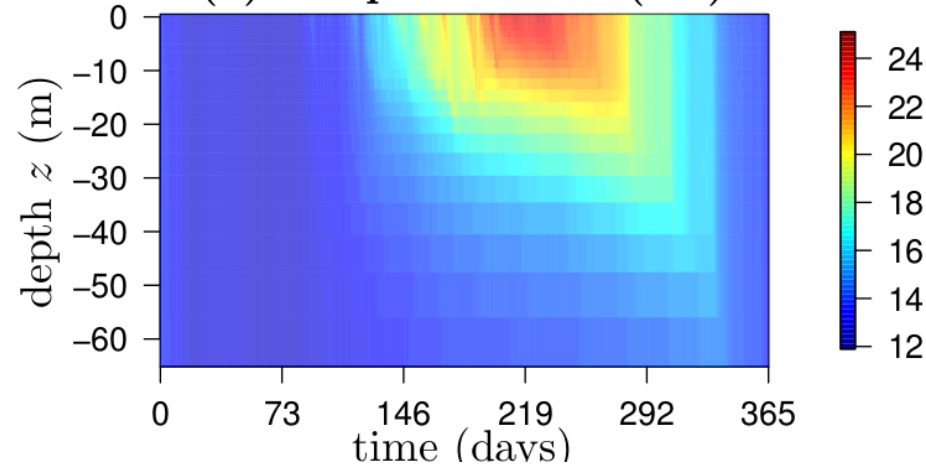
model prediction: first guess



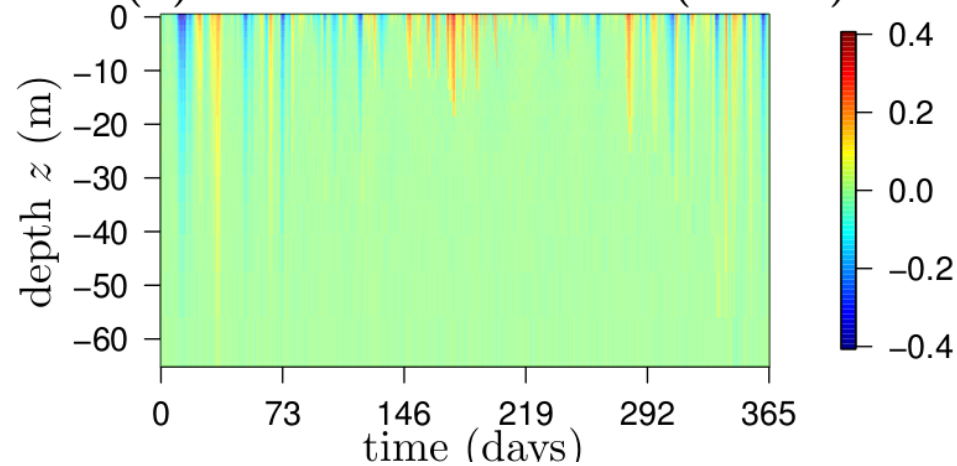
Optimization : Twin experiments

available data

(a) temperature T ($^{\circ}C$)

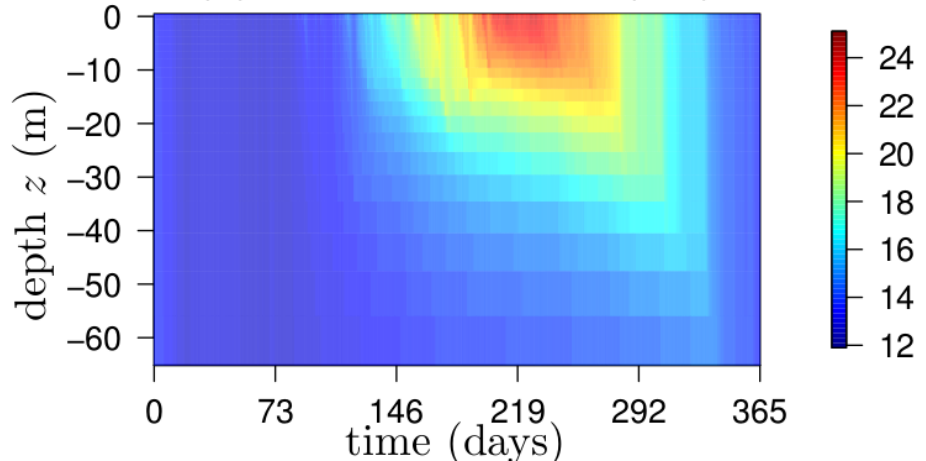


(b) horizontal current v ($m.s^{-1}$)

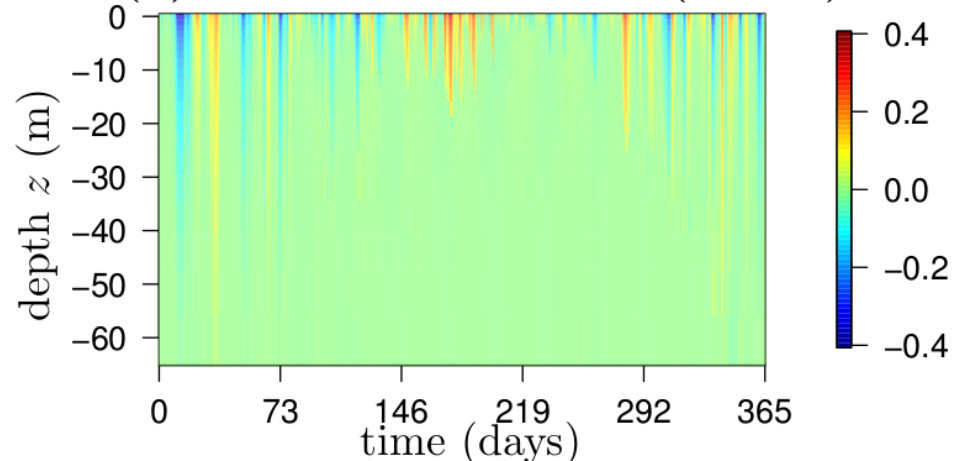


optimized prediction

(g) temperature T ($^{\circ}C$)

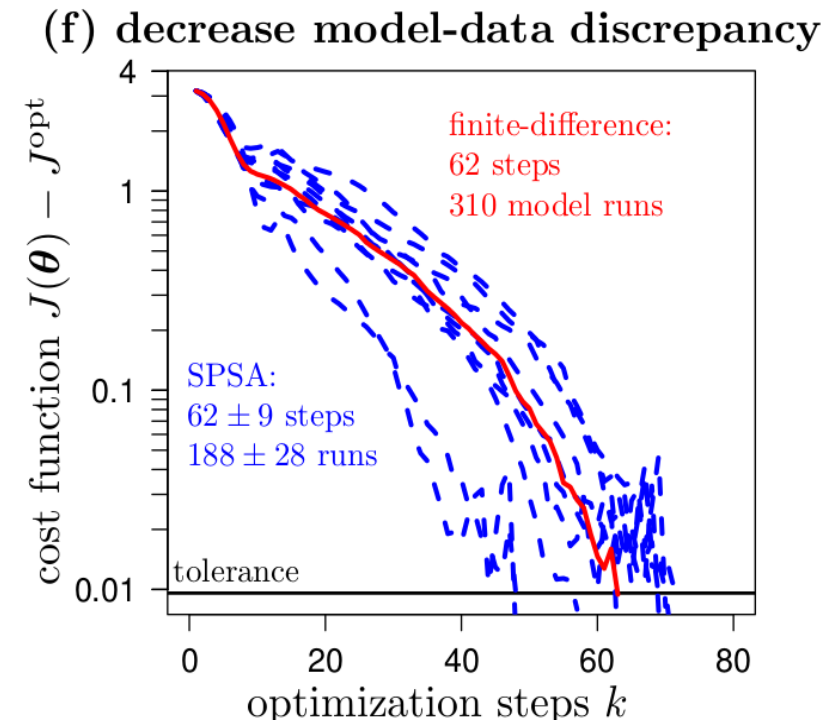
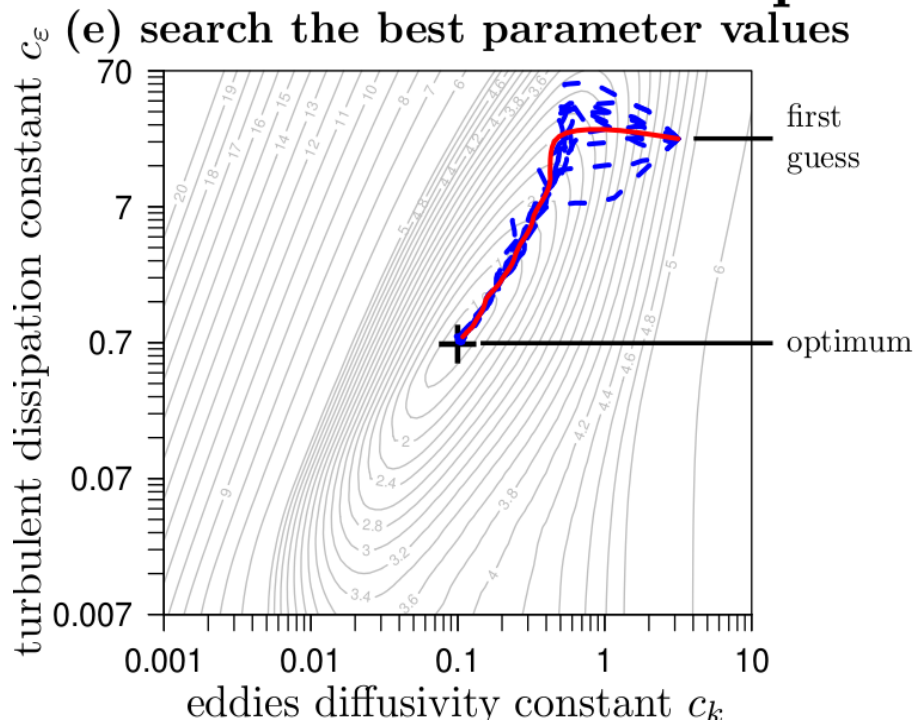


(h) horizontal current v ($m.s^{-1}$)



Optimal search in the control space example in a 2D sub-space

optimization



Cost function and minimization algorithm

(Nesterov Momentum)

$$J(\boldsymbol{\theta}) = \alpha_{uv} \left(\sum_{i=1}^n \left(u_i^{\text{pred}}(\boldsymbol{\theta}) - u_i^{\text{obs}} \right)^2 + \sum_{i=1}^n \left(v_i^{\text{pred}}(\boldsymbol{\theta}) - v_i^{\text{obs}} \right)^2 \right)^{1/2} \\ + \alpha_T \left(\sum_{i=1}^n \left(T_i^{\text{pred}}(\boldsymbol{\theta}) - T_i^{\text{obs}} \right)^2 \right)^{1/2} + \alpha_S \left(\sum_{i=1}^n \left(S_i^{\text{pred}}(\boldsymbol{\theta}) - S_i^{\text{obs}} \right)^2 \right)^{1/2},$$

procedure starting from an arbitrary initial guess of the parameter values $\boldsymbol{\theta}^{(0)}$:

$$\boldsymbol{\theta}^{(k+1)} = \boldsymbol{\theta}^{(k)} - a^{(k)} \mathbf{z}^{(k)}. \quad (2)$$

$a^{(k)}$: step size $\mathbf{z}^{(k)}$ searching direction

$$\mathbf{z}^{(k)} = \beta \mathbf{z}^{(k-1)} + \nabla J(\boldsymbol{\theta}^{(k)} - a^{(k)} \mathbf{z}^{(k-1)}).$$

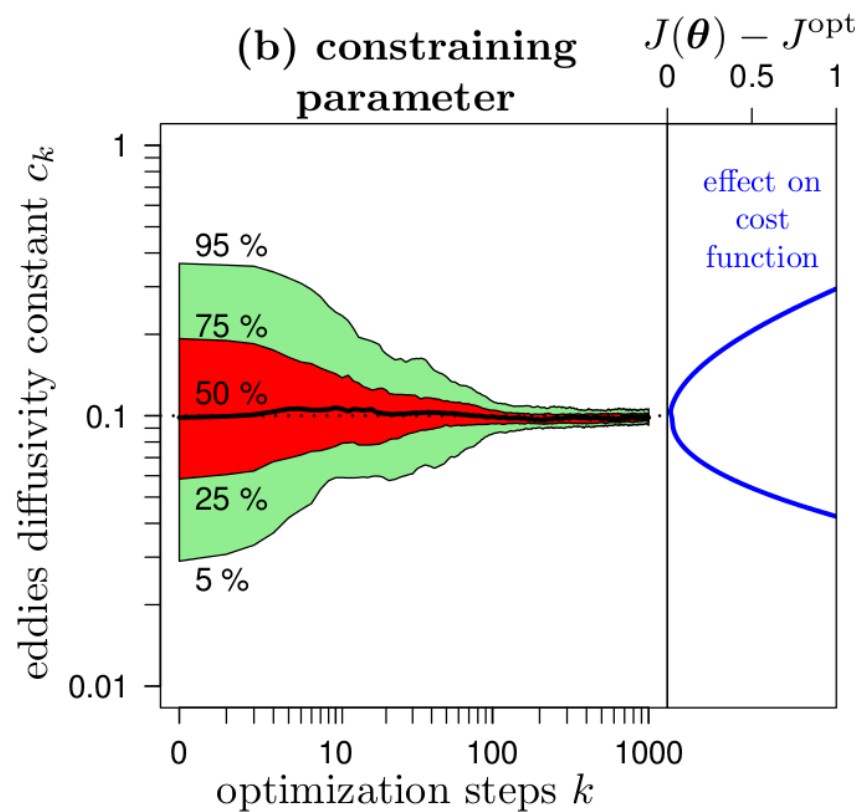
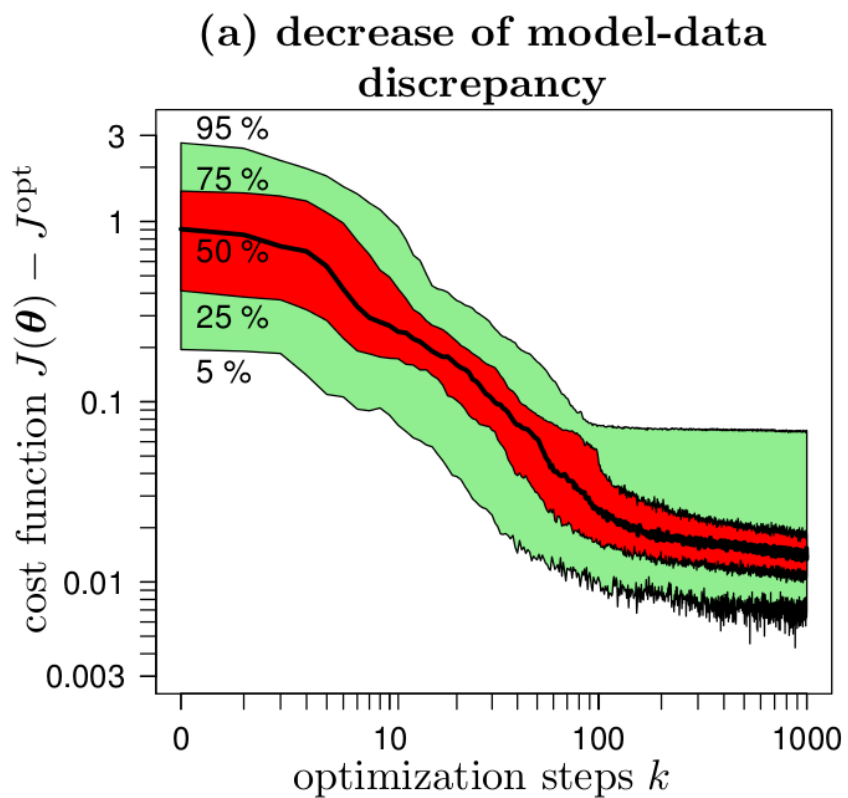
J Gradient estimation

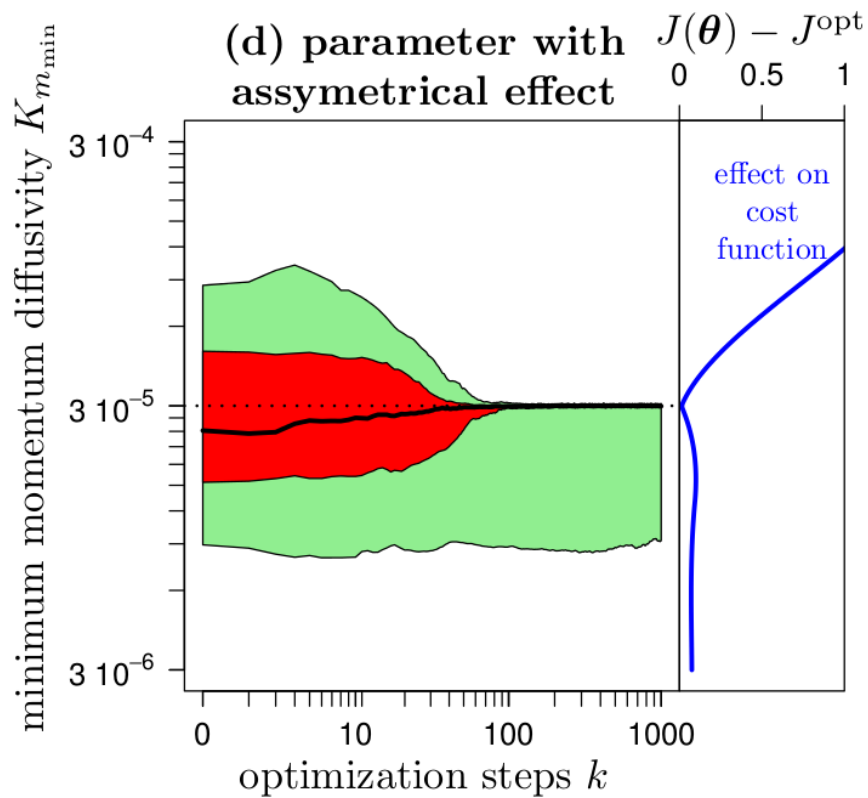
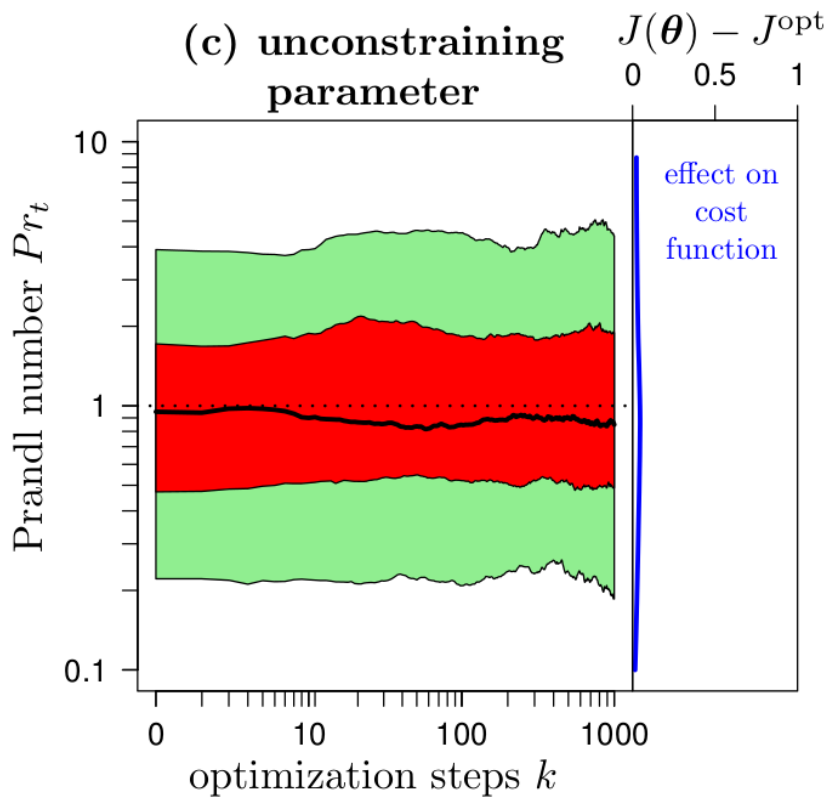
Classical : 1
Parameter
at a time

$$\nabla J(\boldsymbol{\theta}^k) = \begin{pmatrix} \frac{J(\boldsymbol{\theta}^{(k)} + \boldsymbol{\delta\theta}_1^{(k)}) - J(\boldsymbol{\theta}^{(k)} - \boldsymbol{\delta\theta}_1^{(k)})}{2c^{(k)}} \\ \vdots \\ \frac{J(\boldsymbol{\theta}^{(k)} + \boldsymbol{\delta\theta}_i^{(k)}) - J(\boldsymbol{\theta}^{(k)} - \boldsymbol{\delta\theta}_i^{(k)})}{2c^{(k)}} \\ \vdots \\ \frac{J(\boldsymbol{\theta}^{(k)} + \boldsymbol{\delta\theta}_p^{(k)}) - J(\boldsymbol{\theta}^{(k)} - \boldsymbol{\delta\theta}_p^{(k)})}{2c^{(k)}} \end{pmatrix}, \quad \boldsymbol{\delta\theta}_i^{(k)} = c^{(k)} \begin{pmatrix} 0 \\ \vdots \\ 0 \\ 1 \\ 0 \\ \vdots \\ 0 \end{pmatrix} \quad (4)$$

SPSA
simultaneous
Perturbations of
All parameters

$$\nabla J(\boldsymbol{\theta}^k) = \begin{pmatrix} \frac{J(\boldsymbol{\theta}^{(k)} + \boldsymbol{\delta\theta}^{(k)}) - J(\boldsymbol{\theta}^{(k)} - \boldsymbol{\delta\theta}^{(k)})}{2c^{(k)}\Delta_1^{(k)}} \\ \vdots \\ \frac{J(\boldsymbol{\theta}^{(k)} + \boldsymbol{\delta\theta}^{(k)}) - J(\boldsymbol{\theta}^{(k)} - \boldsymbol{\delta\theta}^{(k)})}{2c^{(k)}\Delta_i^{(k)}} \\ \vdots \\ \frac{J(\boldsymbol{\theta}^{(k)} + \boldsymbol{\delta\theta}^{(k)}) - J(\boldsymbol{\theta}^{(k)} - \boldsymbol{\delta\theta}^{(k)})}{2c^{(k)}\Delta_p^{(k)}} \end{pmatrix}, \quad \boldsymbol{\delta\theta}^{(k)} = c^{(k)} \begin{pmatrix} \Delta_1^{(k)} \\ \vdots \\ \Delta_i^{(k)} \\ \vdots \\ \Delta_p^{(k)} \end{pmatrix} \quad (5)$$





Comments and perspectives

- Example of use of SPSA method for a turbulent closure scheme embedded in a one-dimensional vertical model of the ocean.

- Parameters that constrain model predictions are estimated with a high accuracy.

- Some other parameters are well-estimated on average, but with less accuracy(The same as other methods)

- Results are obtained at a relatively low numerical cost.

- Allows to optimize models without an adjoint model costly to derive.

- Method fast enough to allow repetitions, to perform a sensitivity analysis

- Easy to change the optimization problem to solve (model, cost function, available data)

- Possibility to use for boundary conditions fitting or in coupled hydrodynamic-biogeochemical models

Persistence extremal index method

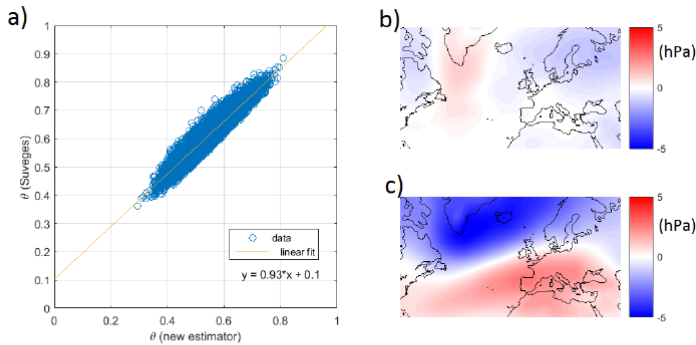


FIGURE 3. a) Scatter plot of $\hat{\theta}_{Su}$ (the Sveges estimator) vs $\hat{\theta}_5$ (the new estimator introduced in this work). Average map of the 5% sea-level pressure patterns such that the residual between $\hat{\theta}_{Su}$ and $\hat{\theta}_5$ are smaller than the 5% percentile (b) or larger (c) than the 95% percentile, for both taking as a threshold the 0.99-quantile of the observable distribution.

Caby, Faranda, Vaienti, Yiou, 2019

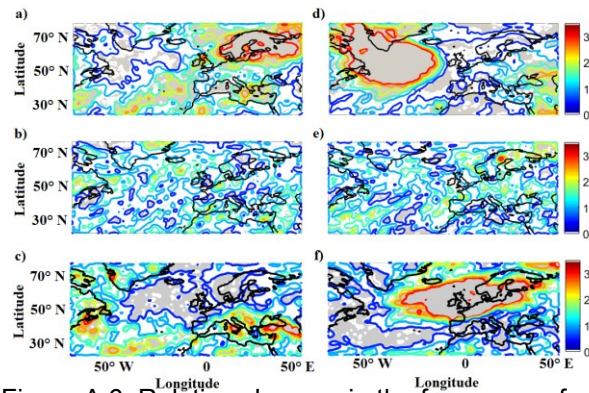
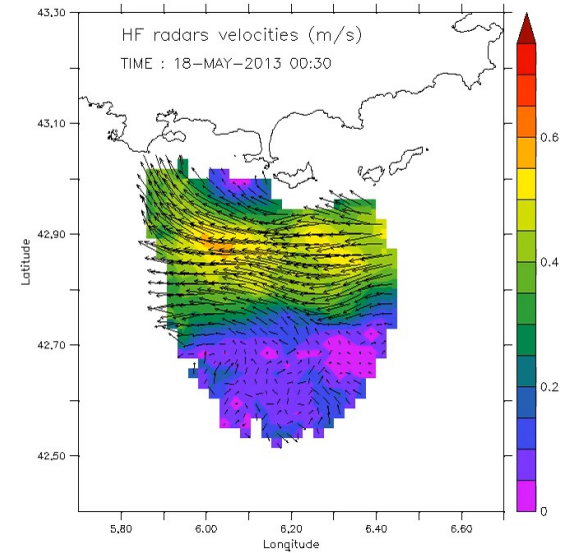
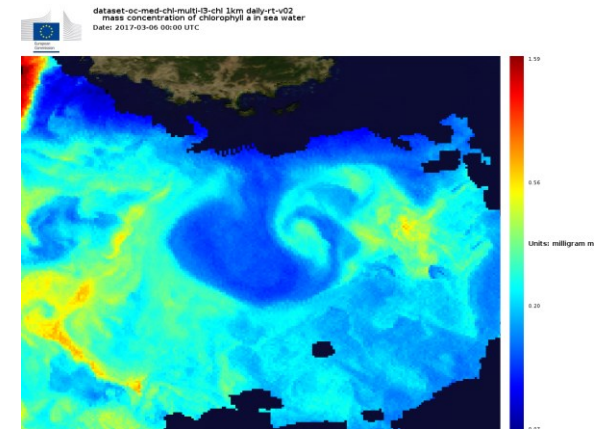


Figure A.6: Relative changes in the frequency of a), d) extreme cold; b), e) extreme wet and c), f) extreme 10m wind events for days with instantaneous dimension beyond the a-c) 0.98 and d-f) 0.02 quantiles of d in the ERA-Interim data. Contours start at 0, with an interval of 0.5; the grey shading shows statistically significant changes. The maps in this gure are generated by MATLAB R2013a.

Faranda, Messori & Yiou 2019



Dumas, Granoull & Gurin

Conclusions

- 3D observations of the marine surface layer in microtidal sea have been started (2DH HF radars + 1V ADP/CTD profilers)
- Sensitivity of the surface mixing layer to eddy viscosity as function of 3D space and time has been investigated (still in a very limited number of situations)
- A fast method for Identification of parameters of turbulent closure models (TKE, KPP, etc) has been proposed (tests in progress)
- A data analysis approach based on dynamical systems has been proposed for sparse data sets to classify events (from rare to extreme) and provide statistics (persistence)
- Ekman model needs to be revisited for high resolution modeling (surface and internal waves, Stokes drift, Langmuir circulations, horizontal variations)

References

- Aldebert C., Koenig G., Baklouti M., Fraunié P. and Devenon J.L. A fast and generic method to identify parameters in complex and embedded geophysical models: the example of turbulent closure in the ocean, *Geophys. Res. Letters*, submitted
- Almelah R.B. and Shriraand V. I.Ocean response to varying wind in models with time and depth dependent eddy viscosity. *J. Fluid Mech.* Submitted
- Bourras, D, H. Branger, G. Reverdin, L. Marié, R. Cambra, L. Baggio, C. Caudoux, G. Caudal, S. Morisset, N. Geyskens, A. Weill, and D. Hauser, 2014. A New Platform for the Determination of Air–Sea Fluxes (OCARINA): Overview and First Results. *J. Atmos. Oceanic Technol.*, 31, 1043-1062.
- Bourras D. et al Air-sea Turbulent Fluxes from Six Experiments with data from a Wave-Following Platform. *JGR Oceans*, in revision
- Caby,T., Faranda, D., Mantica G. , Vaienti S., Yiou P. Generalized dimensions, large deviations and the distribution of rare events *Physica D* submitted
- Caby,T., Faranda, D., Vaienti S., Yiou P. On the computation of the extremal index for time series *Maths DS* submitted
- Faranda D., Alvarez-Castro C., Messori G. 2019. The hammam effect or how a warm ocean enhances large scale atmospheric predictability *Nature communications* 10:1316
- Langlais C., Barnier; B., Molines J-M, Fraunié P., Jacob D. and Kotlarski S. 2009. Evaluation of a dynamically downscaled atmospheric reanalysis in the prospect of forcing long term simulations of the ocean circulation in the Gulf of Lions. *Ocean Modelling* 30, 270-286.
- Leredde Y., Devenon J.-L , I. Dekeyser. 1999. Turbulent viscosity optimized by data assimilation. *Annales Geophysicae*, 17, 1463-1477.
- Leredde Y., Devenon J.-L , I. Dekeyser. 2000. Peut-on optimiser les constantes d'un modèle de turbulence marine par assimilation d'observations ? *C. R. Acad. Sci., Sciences de la Terre et des planètes*, 331:405-412.
- Schaeffer A., Garreau P., Molcard A., Fraunié, P.Seity 2011. Y. Influence of high resolution wind forcing on the gulf of Lions hydrodynamic modelling, *Ocean Dynamics* vol61, 11, pp1823-1844.DOI: 10.1007/s10236-011-0442-3.
- Sentchev A., Forget P., Fraunié P. 2017. Surface current dynamics under sea breeze conditions observed by simultaneous HF radar, ADCP and drifter measurements. *Ocean Dynamics*, 67, 3-4
- Shrira V, Forget P. 2015, On the Nature of Near-Inertial Oscillations in the Uppermost Part of the Ocean and a Possible Route towards HF Radar Probing of Stratification, *J. Physical Oceanogr.*, 45, 10, 2660-2678
- Verdier-Bonnet C. , P. Angot, P. Fraunié, M. Coantic, 1999. Three dimensional modelling of coastal circulations with different closures, *J. Marine Systems*, vol 21, 1-4, 321-339,
- Xing, A.M. Davies, P. Fraunié, 2004. Model studies of near-inertial motion on the continental shelf off northeast Spain : a 3D/2D model comparison study, 24p, *J.Geophys. Res.*, 109, C01017